Marked 18-Fuorine-Fluorodeoxyglucose (FDG) Avidity of an Intrapulmonary Typical Carcinoid Tumor Manifesting as a Bronchocele in an Asymptomatic Middle-Aged Woman

Authors' Contribution:
Study Design A
Data Collection B
Statistical Analysis C
Data Interpretation D
Manuscript Preparation E
Literature Search F
Funds Collection G

AEF 1 **Camila Saadé-Yordán**
D 1 **Edward McBurney-Henriquez**
B 2 **Ricardo González-Santoni**
D 3 **Carmen Gurrea-Rosas**
B 4 **José Montalvo-Fitzpatrick**
DEF 1 **José A. Maldonado-Vargas**

1 Department of Diagnostic Radiology, University of Puerto Rico School of Medicine, San Juan, Puerto Rico
2 Department of Family Medicine, University of Puerto Rico School of Medicine, San Juan, Puerto Rico
3 Department of Pathology, Cardiovascular Center of Puerto Rico and The Caribbean, San Juan, Puerto Rico
4 Department of Cardiothoracic Surgery, Cardiovascular Center of Puerto Rico and The Caribbean, San Juan, Puerto Rico

Corresponding Author: Camila Saadé-Yordán, e-mail: csaade15@gmail.com, camila.saade@upr.edu
Conflict of interest: None declared

Patient: **Female, 67**
Final Diagnosis: **Pulmonary carcinoid tumor**
Symptoms: **Abnormal shadow on Chest X-ray**
Medication: **—**
Clinical Procedure: **Surgery – left upper lobe lobectomy**
Specialty: **Radiology**

Objective: **Unusual clinical course**
Background: Intrapulmonary carcinoid tumors (ICTs) are malignant, slow-growing tumors classified as either: i) typical, less aggressive, well-differentiated tumors or ii) atypical, more aggressive, poorly-differentiated tumors. Most typical carcinoid tumors originate in the central airway and present with symptoms related to bronchial obstruction. In contrast, atypical carcinoids tend to occur more peripherally and are generally detected incidentally as a solitary pulmonary nodule (SPN). Typical carcinoid tumors usually do not exhibit increased metabolic activity on positron emission tomography with 18-fuorine-fluorodeoxyglucose (FDG PET) as would be expected for malignant tumors. In this case report, we present an unusual case of a typical, well-differentiated, peripheral carcinoid tumor showing marked FDG avidity manifesting as a bronchocele. We discuss the differential diagnoses and describe the diagnostic approach undertaken in this exemplary case of a common clinical problem.
Case Report: A left upper-lobe, peripheral, 2-cm pulmonary nodule was incidentally identified on chest radiography of an asymptomatic 67-year-old female patient. Chest CT scan with intravenous (IV) contrast showed a noncalcified nodule with a branching pattern. Further evaluation with FDG PET/CT scan demonstrated marked FDG avidity. Post-surgical biopsy revealed a typical, well-differentiated, intrapulmonary carcinoid tumor.
Conclusions: Carcinoid tumors of the lung remain a diagnostic challenge for primary care physicians and radiologists due to their diverse clinical and radiological presentations. Peripheral carcinoid tumors usually present as an asymptomatic peripheral, solitary, pulmonary nodule, but isolated peripheral bronchocele has been described, as in our case. In addition, caution must be taken when utilizing FDG PET/CT scan for the evaluation of a possible lung carcinoid tumor, as an accurate value range of FDG uptake for diagnosis of these tumors has not been defined.

MeSH Keywords: **Carcinoid Tumor • Fluorodeoxyglucose F18 • Lung Neoplasms • Solitary Pulmonary Nodule**

Full-text PDF: https://www.amjcaserep.com/abstract/index/idArt/906678

Background

A solitary pulmonary nodule (SPN) is found on chest radiography or computed tomography (CT) in more than 150 000 patients each year in the United States [1,2]. This presents a diagnostic dilemma since the differential diagnosis is very broad and includes both benign and malignant lesions. Intrapulmonary carcinoid tumors (ICTs) are a relatively uncommon cause of a SPN and represent about 1–3% of all lung cancers.

Carcinoid tumors are indolent, malignant neoplasms derived from neuroendocrine precursor-type cells. They are most commonly found in the gastrointestinal tract, although it is estimated that 20–30% of neuroendocrine tumors arise in the bronchial tree [3]. ICTs are uncommon when compared to other primary lung malignancies, representing only 1–3% [4]. Reports in the literature show the central airway predominance for these tumors, thought to be due to the high likelihood of undergoing diagnostic evaluation owing to the symptomatic presentation related to bronchial obstruction, such as recurrent infections, shortness of breath, hemoptysis, wheezing, and cough [5]. The most commonly described CT characteristic of intrapulmonary carcinoid tumors is an endobronchial-based, avidly-enhancing, soft tissue mass with lobulated or spiculated margins. Eccentric calcifications are common [6]. Tumor size ranges from 2 to 3 cm [7]. Significant enhancement after intravenous contrast administration reflects the hypervascularity of these malignant tumors [5]. CT imaging findings associated with bronchial obstruction include hyperlucency related to air trapping, atelectasis, and bronchiectasis distal to the lesion. However, recent studies have demonstrated a predominance of ICTs located peripherally [3,5]. Peripheral carcinoid tumors are usually detected incidentally as a solitary pulmonary nodule, and symptoms related to tumor obstruction are usually absent [5].

ICTs have been traditionally classified into typical (TC) or atypical (AC), based on their biological behavior and histological characteristics [8]. While typical carcinoids are usually well-differentiated and slow-growing tumors, atypical carcinoids tend to be more aggressive and poorly differentiated. No definite association has been shown between their biological behavior and tumor locality. Nonetheless, Travis and Pusceddu et al. have reported that well-differentiated typical carcinoid tumors show a predilection for a central airway location, while atypical carcinoids favor a peripheral location [3,7].

ICTs have been notoriously described as tumors with low metabolism and slow growth. Therefore, they have been regarded as tumors showing low FDG uptake in FDG PET/CT imaging [9]. Recently, however, multiple investigations have concurred that these tumors show increased FDG uptake values, as would be expected for malignant tumors [10]. Additionally, a direct correlation of FDG uptake values with the biological behavior of the tumor has been determined, as atypical carcinoids show higher FDG uptake values when compared to lower-grade intrapulmonary carcinoid tumors [11]. Interestingly, Gasparri et al. demonstrated no significant difference between the mean
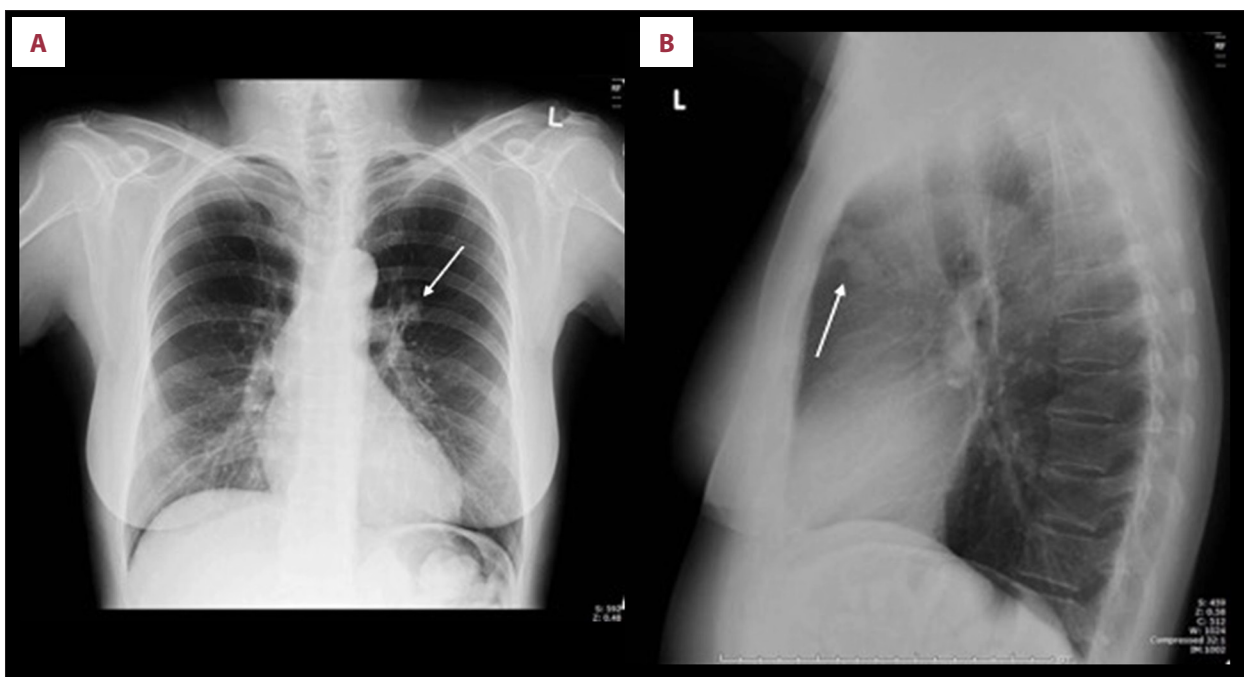

Figure 1. (**A**) PA and (**B**) lateral chest radiographs show a retrosternal nodular soft tissue density projecting in the left upper lung zone anteriorly (arrow).
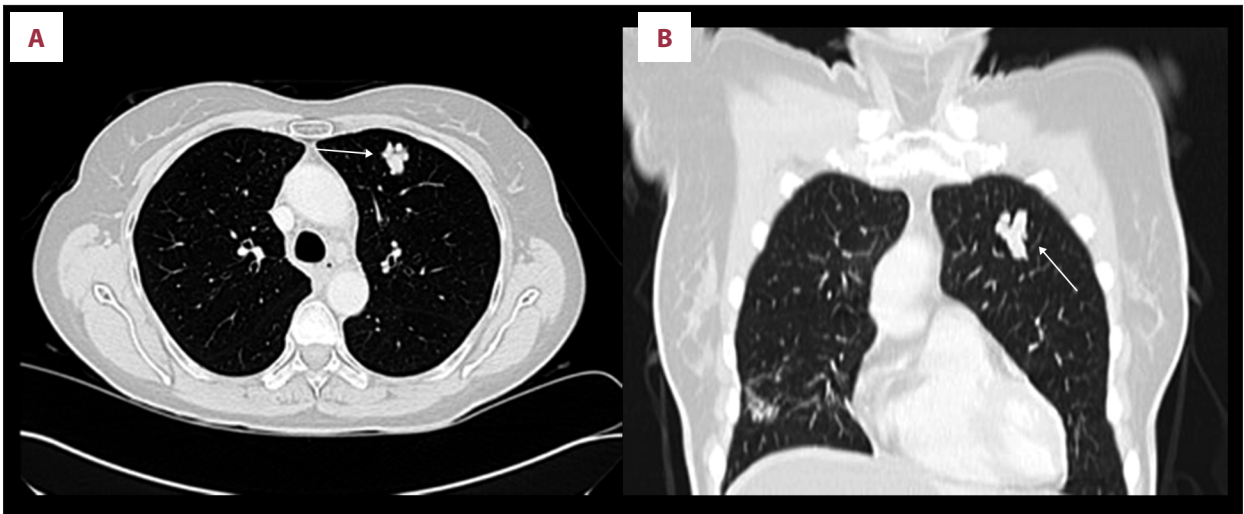
Figure 2. (**A**) Axial and (**B**) coronal lung window CT images show a left upper-lobe branching opacity, consistent with a bronchocele (arrow). Atelectasia is also present in the right lower lobe (**B**).

standardized uptake values (SUV) of typical versus atypical carcinoid tumors [12].

Although relatively infrequent, ICTs may produce ectopic hormonal substances and metabolically active peptides due to their neuroendocrine origin. Excessive production of hormones by these tumors results in unique clinical syndromes, depending on the type of molecule produced, aiding in the diagnosis of these tumors. These are known as paraneoplastic endocrine syndromes (PES) and include: adrenocorticotropic hormone (ACTH) or corticotropin-releasing hormone (CRH) production resulting in Cushing's syndrome, abnormal antidiuretic hormone (ADH) secretion resulting in syndrome of inappropriate antidiuretic hormone secretion (SIADH), and hypercalcemia caused by parathyroid hormone-related secretion [13]. Carcinoid syndrome (episodic diarrhea, flushing, wheezing, carcinoid heart disease) caused by an ICT may result from the release of high concentrations of serotonin, although it is uncommon [13]. Due to the notorious increased expression of somatostatin receptors in neuroendocrine tumors, functional imaging with somatostatin receptor scintigraphy can be performed for the detection and localization of these tumors [14,15].

Case Report

A 67-year-old female patient with no significant past medical history presented with an incidental finding on a routine chest radiograph. A nodular radiopacity was suggested in the projection of the left hilum, somewhat obscured by the pulmonary markings and overlying the seventh (7th) rib (Figure 1A). A lateral projection was also obtained, which confirmed the presence of a pulmonary nodule in the anterior segment of the left upper lobe (Figure 1B). The patient denied any recent history

Figure 3. Soft tissue window axial CT scan demonstrates left upper-lobe nodular opacity with an average HU attenuation value of 66 (arrow).

of cough, hemoptysis, shortness of breath, or recurrent pneumonias. She also denied history of first-hand smoking. A CT scan of the chest after the administration of IV contrast was performed for further characterization. A non-contrast image acquisition was not obtained. The contrast-enhanced chest CT showed a smoothly marginated, noncalcified, lobulated nodule with a branching contour in the periphery of the anterior segment of the left upper lobe (Figures 2A, 2B, 3). There was no surrounding parenchymal hyperlucency. The nodule showed no avid enhancement, with a relatively homogeneous attenuation after intravenous contrast administration, comparable to that of muscle, with a mean Hounsfield unit (HU) value of 66 (Figure 3). A whole-body FDG PET/CT scan was performed and a hypermetabolic multilobulated left upper lobe density was identified with an elevated maximum SUV of 3.42. No other FDG-avid lesions were detected. Symptoms associated with
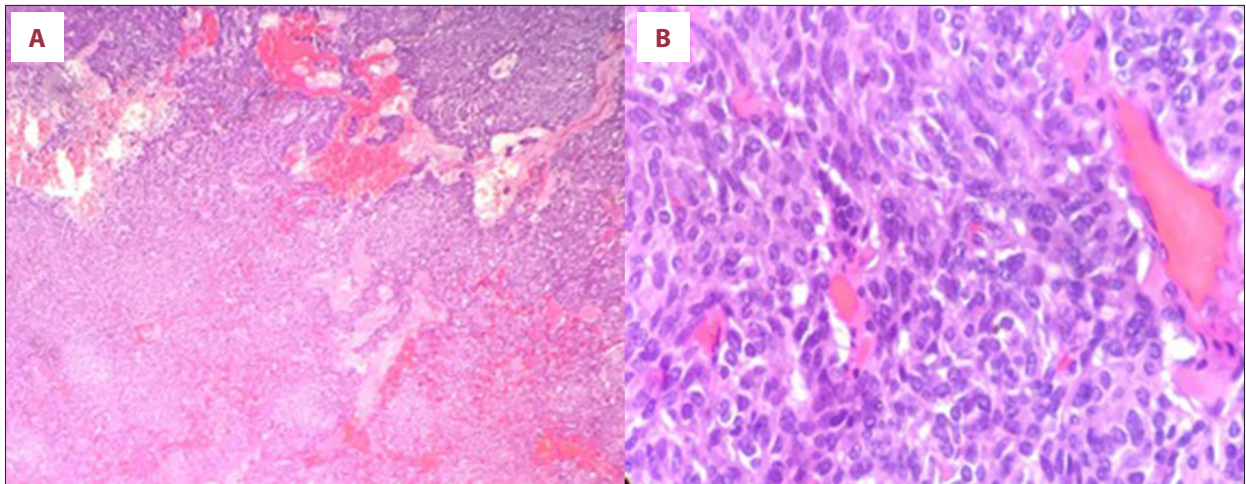
Figure 4. (**A**) Low-power view showing solid masses of monotonous small round cells with peripheral palisading. (**B**) High-power view showing monotonous small round cells with moderate finely granular cytoplasm, and small nucleoli, with "salt and pepper"-like chromatin. Mitoses are rare. H&E stain.

the presence of a possible paraneoplastic syndrome, including diarrhea, flushing, or any metabolic disturbance, were absent. Routine laboratory values were noncontributory.

A surgical biopsy approach was undertaken and a left upper-lobe lobectomy was performed. Multiple hilar, paratracheal, and mediastinal lymph nodes were sampled for evaluation. Gross pathology described a mass in the upper segment of the left upper lobe, measuring 2.5×2.3×1.5 cm. Histology revealed monotonous small round cells with moderate finely granular cytoplasm, small nucleoli, with "salt and pepper"-like chromatin (Figure 4A, 4B). The histology was consistent with a well-differentiated neuroendocrine carcinoma. The overlying pleura was intact. Sampled lymph nodes were negative for malignancy. The patient recovered well from surgical intervention. The post-operative course has been unremarkable, without evidence of tumor recurrence or metastatic disease.

Discussion

The presence of a nodular radiopacity during routine evaluation of the chest with radiography is a common finding in clinical practice. The first step is to determine if in fact a true pulmonary nodule exists, since artifacts, objects outside the patient, and non-pulmonary lesions (e.g., nipple, skin mole, bone island) can mimic a pulmonary nodule. In most instances, whenever a single frontal projection is obtained, the exact anteroposterior position of a radiopacity will be unknown. A lateral view of the chest allows for accurate localization of the radiopacity in question and must therefore be part of every complete radiographic evaluation of the chest if the patient's clinical condition permits upright positioning. In our case, the nodular radiopacity was more conspicuous on the lateral view

and was confirmed to be a true pulmonary nodule localized in the anterior segment of the left upper lobe.

Once the presence of a pulmonary nodule has been established on chest radiography, integration of clinical findings such as patient age, symptoms such as fever or hemoptysis, risk factors such as cigarette smoking or occupational exposure, and recent travel history is paramount. Comparison with prior radiographs is always useful since more than two-year stability of a pulmonary nodule is suggestive of a benign process. This "two-year rule", however, must be used with caution since some lesions, including typical carcinoids and low-grade adenocarcinomas, occasionally appear to be stable for 2 or more years [2]. If prior radiographs are not available, if the long-term stability of the nodule cannot be established, or if there is clinical suspicion of the presence of neoplasia, evaluation with chest CT must follow. CT is superior to chest radiography in the characterization of pulmonary nodules, allowing for better determination of their imaging characteristics including: size, presence and type of calcification (e.g., popcorn-type *vs.* concentric), density (e.g., fat), morphology (e.g., round *vs.* branching), and nodule-lung interface (e.g., smooth *vs.* spiculated).

In our case, the CT revealed an important morphologic characteristic of the nodule: a branching pattern consistent with a bronchocele. Bronchoceles represent dilated airways filled with impacted intra-luminal material, which may be neoplastic cells rather than only inspissated mucus [16]. They can result from obstructive or non-obstructive etiologies. Among the most common non-obstructive etiologies is cystic fibrosis and allergic bronchopulmonary aspergillosis (ABPA), while obstructive causes include bronchial atresia and neoplasia. Below, we discuss the rationale we utilized to generate a differential diagnosis of our case after taking into consideration radiological and clinical data.

One possible etiology that was considered, as a disease presenting with a bronchocele, was cystic fibrosis, which is a multisystemic congenital disorder of impaired ciliary motility. The pulmonary hallmark characteristics in cystic fibrosis are bronchiectasis secondary to lung damage and airway wall thickening [17]. With disease progression, bronchial mucus plugging develops, resulting in bronchoceles relatively early in life. Additional findings in cystic fibrosis include peribronchial interstitial thickening, air trapping, emphysema, and history of recurrent pulmonary infections [17]. The first and most obvious fact in our case that argued against a diagnosis of cystic fibrosis was the lack of a history of recurrent pulmonary infections. Additionally, chest CT in our case lacked all the above-described findings commonly seen in patients with cystic fibrosis, including a more diffuse pattern of lung disease.

ABPA is a disease commonly encountered as a complication in patients with asthma and cystic fibrosis. It is believed to be caused by a hypersensitivity response to *Aspergillus* species in the bronchial lumen [18]. Characteristic CT findings include central bronchiectasis, high-attenuation mucus, air trapping, and centrilobular nodules [18]. Multiple mucus-filled bronchoceles have also been described [19]. High-attenuation mucous plugging is considered the most characteristic finding of ABPA [18]. Unfortunately, in our case a non-contrast CT scan was not obtained to determine the intrinsic attenuation value of the opacity and to determine the degree of enhancement. However, relatively high attenuation of the opacity (mass or bronchocele) was documented, with mean HU value of 66. This could have been attributed to high-attenuation mucus, as can be seen with ABPA, or a mass showing an intermediate degree of contrast enhancement. Although cases of ABPA in patients without asthma have been described by Amin et al. (2008) [19], it is not the usual presentation. In the present study, the patient did not have a history of asthma or cystic fibrosis. Also, the absence of central bronchiectasis, air trapping, or additional nodularities helped us rule out this diagnosis. Moreover, our patient's laboratory results did not show peripheral blood eosinophilia, which can be present in ABPA.

Obstructive causes of a bronchocele include bronchial atresia and obstructive neoplasm. Bronchial atresia is a developmental airway anomaly resulting from focal interruption of the airway [20]. Associated development of mucus impaction distal to the stenotic airway, as well as hyperlucency adjacent to surrounding lung parenchyma, are considered pathognomonic for bronchial atresia [20]. Distal hyperlucency is thought to be caused by collateral ventilation resulting in air trapping [20]. Bronchial atresia can be asymptomatic and it is most commonly located in left upper lobe, as in our case [21]. Average age at presentation is 17 years old [21]. Bronchial atresia is a diagnosis that could have been strongly considered in our case given the similar CT characteristics, including a peripherally located left upper-lobe

bronchocele and the relative absence of other CT findings that would have been present in the etiologies previously described.

An obstructive neoplasm, such as a bronchogenic carcinoma and intrapulmonary carcinoid tumors, can mechanically impair the normal bronchial clearance, causing epithelial secretions to become trapped distally [22]. Bronchocele secondary to bronchogenic carcinoma is not a common finding. However, when present, the tumor is usually centrally located [22]. Similarly, as described previously, endobronchial carcinoid tumors presenting in association to a bronchocele are usually located in the central airway. However, peripheral carcinoids are most commonly detected incidentally as a solitary pulmonary nodule. CT findings of a centrally based neoplasm include a hilar mass with or without mediastinal lymphadenopathy [22]. Contrast-enhanced CT scanning would help with further characterization, as the tumor portion would significantly enhance. In our case, a peripheral left upper-lobe bronchocele was identified without an evident mass and no considerable contrast-enhancing component was observed after contrast administration. Additionally, it would be expected for a lesion causing obstruction of the airways to present with symptoms related to bronchial obstruction, which were absent in our patient.

In our case, determining the enhancing characteristics of the incidentally discovered opacity was difficult, as an unenhanced study was not obtained for reference. Moreover, no distinct mass or nodule was identified to indicate its exact attenuation value. A mean attenuation value of 66 HU was measured, indicating no avid enhancement. Attenuation value could have been attributed to inspissated, high-attenuation mucus related to ABPA.

To this point, the etiology of the incidental discovery of a peripheral, poorly enhancing bronchocele was uncertain and FDG PET/CT scanning was used to aid in the diagnosis, as recommended by the American College of Radiology Appropriateness Criteria [ACR-AC]. The increased metabolic activity of the bronchocele, which demonstrated elevated SUV of 3.42 in FDG PET/CT scan, mandated that we strongly considered a malignant tumor. Other FDG-avid inflammatory lesions and granulomatous diseases, such as sarcoidosis, tuberculosis, and fungal infections, were also considered [23].

The workup proceeded through a surgical and pathological diagnostic approach, whereby a well-differentiated carcinoid tumor was unexpectedly diagnosed. The elevated SUV of the typical carcinoid tumor in this case is in keeping with recent studies that demonstrate considerable FDG avidity of ICTs. Additionally, the elevated SUV was even more surprising after post-surgical histological diagnosis of a well-differentiated, typical carcinoid tumor was confirmed, as recent studies have demonstrated lower FDG values for typical carcinoids when compared to atypical carcinoids.

Conclusions

It is important to understand that ICTs can present with a wide variety of clinical and radiological findings, ranging from a symptomatic, centrally-located, avidly-enhancing endobronchial mass related to distal atelectasis, air trapping, or mucoid impaction to an asymptomatic, isolated, peripheral bronchocele showing no avid contrast enhancement, as in our case. In addition, we must be aware of the varied FDG uptake values of ICTs when characterizing an intrapulmonary opacity with FDG PET/CT scanning, as a definite range of values has not yet been established.

References:

1. Tan BB, Flaherty KR, Kazerooni EA, Iannettoni MD: The solitary pulmonary nodule. Chest, 2003; 123: 89S–96S

2. Ost D, Fein AM, Feinsilver SH: Clinical practice. The solitary pulmonary nodule. N Engl J Med, 2003; 348: 2535–42

3. Pusceddu S, Lo Russo G, Macerelli M et al: Diagnosis and management of typical and atypical lung carcinoids. Crit Rev Oncol Hematol, 2016; 100: 167–76

4. Correia S da S, Pinto C, Bernardo J: [Pulmonary carcinoid: Analysis of a single institutional experience and prognostic factors]. Acta Med Port, 2014; 6: 749–54 [in Portuguese]

5. Meisinger QC, Klein JS, Butnor KJ et al: CT features of peripheral pulmonary carcinoid tumors. Am J Roentgenol, 2011; 197: 1073–80

6. Jeung M-Y, Gasser B, Gangi A et al: Bronchial carcinoid tumors of the thorax: Spectrum of radiologic findings. Radiographics, 2002; 22: 351–65

7. Travis WD: Advances in neuroendocrine lung tumors. Ann Oncol, 2010; 21: vii65–71

8. Naalsund A, Rostad H, Strom EH et al: Carcinoid lung tumors – incidence, treatment and outcomes: a population-based study. Eur J Cardiothorac Surg, 2011; 39: 565–69

9. Erasmus JJ, McAdams HP, Patz EFJ et al: Evaluation of primary pulmonary carcinoid tumors using FDG PET. Am J Roentgenol, 1998; 170: 1369–73

10. Tatci E, Ozmen O, Gokcek A, Biner IU et al: 18F-FDG PET/CT rarely provides additional information other than primary tumor detection in patients with pulmonary carcinoid tumors. Ann Thorac Med, 2014; 9: 227–31

11. Stefani A, Franceschetto A, Nesci J et al: Integrated FDG-PET/CT imaging is useful in the approach to carcinoid tumors of the lung. J Cardiothorac Surg, 2013; 8: 223.

12. Gasparri R, Rezende GC, Fazio N et al: Fluorodeoxyglucose positron emission tomography in pulmonary carcinoid tumors. Q J Nucl Med Mol Imaging, 2015; 59: 446–54

13. Gustafsson BI, Kidd M, Chan A et al: Bronchopulmonary neuroendocrine tumors. Cancer, 2008; 113: 5–21

14. Kvols LK, Brown ML, O'Connor MK et al: Evaluation of a radiolabeled somatostatin analog (I-123 octreotide) in the detection and localization of carcinoid and islet cell tumors. Radiology, 1993; 187: 129–33

15. Belhocine T, Foidart J, Rigo P et al: Fluorodeoxyglucose positron emission tomography and somatostatin receptor scintigraphy for diagnosing and staging carcinoid tumours: Correlations with the pathological indexes p53 and Ki-67. Nucl Med Commun, 2002; 23: 727–34

16. Aronberg DJ, Sagel SS, Jost RG, Levitt RG: Oat cell carcinoma manifesting as a bronchocele. Am J Roentgenol, 1979; 132: 23–25

17. Wielputz MO, Eichinger M, Biederer J et al: Imaging of cystic fibrosis lung disease and clinical interpretation. Rofo, 2016; 188: 834–45

18. Agarwal R, Khan A, Gupta D et al: An alternate method of classifying allergic bronchopulmonary aspergillosis based on high-attenuation mucus. PLoS One, 2010; 5: e15346

19. Amin MU, Mahmood R: Multiple bronchoceles in a non-asthmatic patient with allergic bronchopulmonary aspergillosis. J Pak Med Assoc, 2008; 58: 514–16

20. Wang Y, Dai W, Sun Y et al: Congenital bronchial atresia: Diagnosis and treatment. Int J Med Sci, 2012; 9: 207–12

21. Gipson MG, Cummings KW, Hurth KM: Bronchial atresia. Radiographics, 2009; 29: 1531–35

22. Martinez S, Heyneman LE, McAdams HP et al: Mucoid impactions: Finger-in-glove sign and other CT and radiographic features. Radiographics, 2008; 28: 1369–82

23. Chang JM, Lee HJ, Goo JM et al: False positive and false negative FDG-PET scans in various thoracic diseases. Korean J Radiol, 2006; 7: 57–69